Linear-polarization analysis using triple axis spectrometers and PTAX science highlights

Masaaki Matsuda

PTAX point of contact

Spectroscopy group

Oak Ridge National Laboratory

ORNL is managed by UT-Battelle, LLC for the US Department of Energy

Polarized Neutron Diffraction and Spectroscopy: Applications to Quantum Materials
March 30-April 2, 2026

Old days at PTAX/HB-1

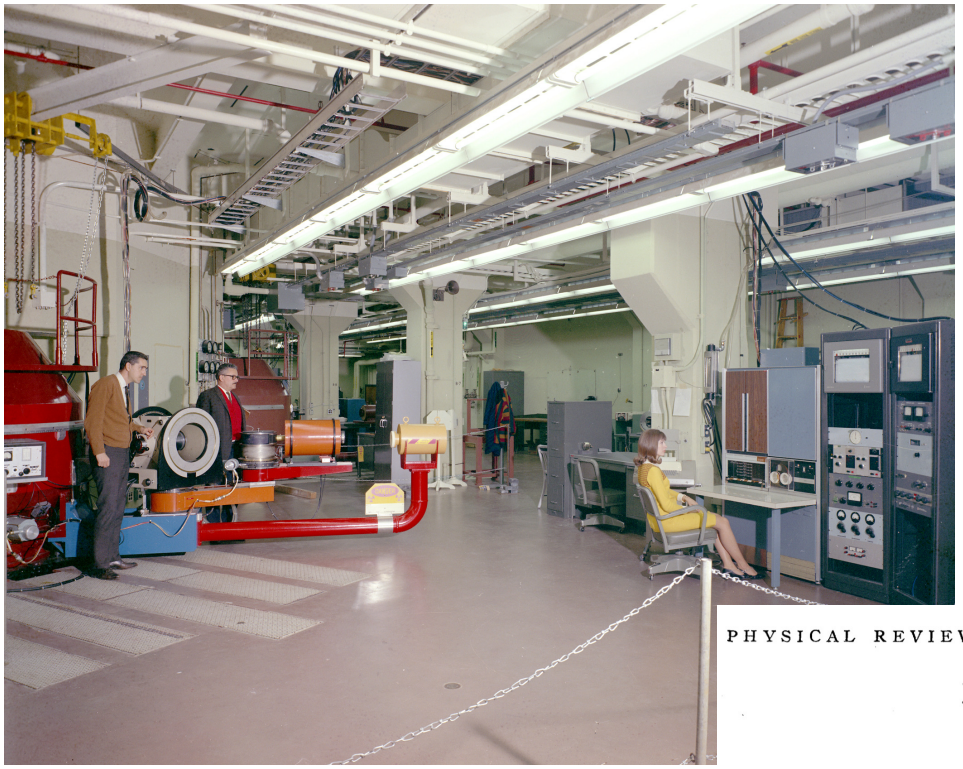

- HB-1 was used by Moon and Koehler for pioneering work in neutron polarization analysis in the late 1960's.

PHYSICAL REVIEW VOLUME 181, NUMBER 2 10 MAY 1969

Polarization Analysis of Thermal-Neutron Scattering*

R. M. Moon, T. Riste,† and W. C. Koehler
Solid State Division, Oak Ridge National Laboratory, Oak Ridge, Tennessee 37830
(Received 30 December 1968)

A triple-axis neutron spectrometer with polarization-sensitive crystals on both the first and third axes is described. The calculation of polarized-neutron scattering cross sections is presented in a form particularly suited to apply to this instrument. Experimental results on nuclear incoherent scattering, paramagnetic scattering, Bragg scattering, and spin-wave scattering are presented to illustrate the possible applications of neutron-polarization analysis.

PTAX/HB-1 at HFIR

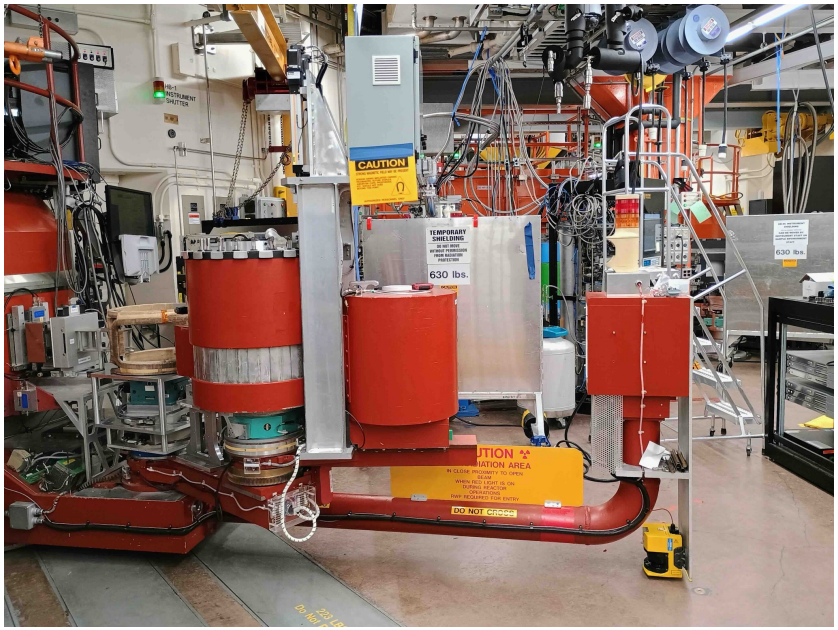

PTAX: 100% polarized mode since January 2022

Heusler (Cu_2MnAl) monochromator and analyzer

(flipping ratio: ~15 at 13.5 meV and ~10 at 30.5 meV)

Beam size: ~30 mm X 30 mm

Energy: Ei 10 – 45 meV (1.35 – 2.86 Å)

Ef 13.5 meV (2.46 Å) and 30.5 meV (1.64 Å)

- Hard condensed matter physics
- Versatile instrument for both diffraction (~70%) and inelastic measurements (~30%)
- Parametric study in magnetic field, high/low temperatures, pressure, …..
  (Good complement to HYSPEC at SNS)

Sample environments

- Temperature: 30 mK – 1873 K
- Magnetic field: 6 T/8 T (vertical): 1.5 K – 300 K
- Electric field: 10 kV, 1.5 K – 300 K
- Pressure: 1.8 GPa with piston cell, 0.3 – 500 K
- Uniaxial pressure (strain)

Ongoing upgrade

Heusler monochromator and analyzer (2020-)

New focusing monochromator and analyzer for better beam flux and spin polarization

Purchased from LLB-Saclay

Analyzer

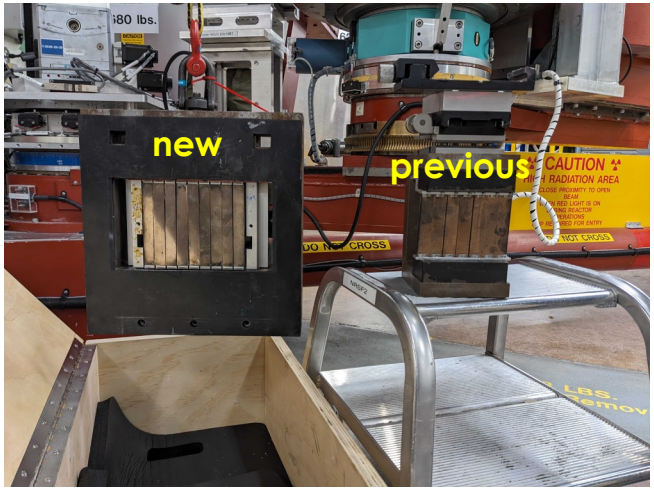

- Variable horizontal focusing
- Installed last month

- Flat
- Small

Monochromator

current

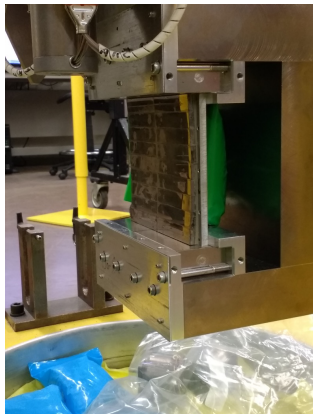

- Inadequate Heusler crystals
- Low flipping ratio
- Low intensity
- Fixed vertical focus

new

- Variable vertical focusing
- Redesign in progress

Heusler polarizer

Pros

- **Maintenance free**
- **Time independent polarization**
- **No need for extra space**
- **High magnetic field experiments feasible**
- **Reasonably good polarization in a wide energy range**

Cons

- **Difficult to obtain high quality crystals**
- **Strong lambda/2 contamination**

Options for polarization analysis on PTAX

Helmholtz coils

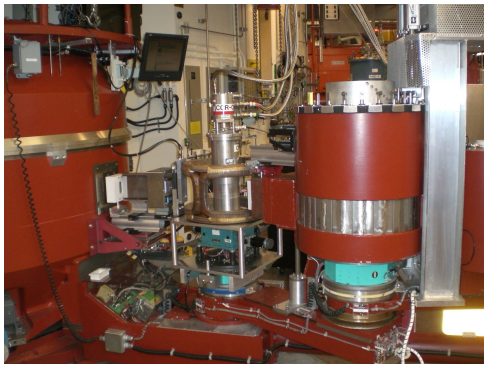

Full polarization analysis - Longitudinal analysis

Half polarization analysis - Chirality

~45 %

6T/8T asymmetric magnet

Half and full polarization analysis - Ferromagnets

~15 %

Wollaston Prism

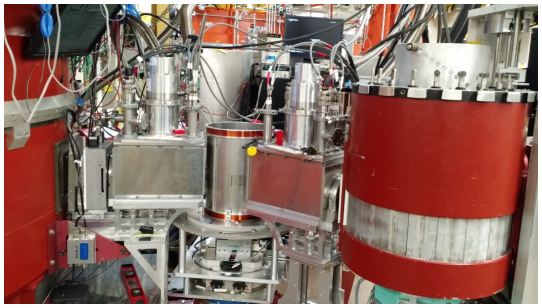

Larmor diffraction – high Q resolution
Neutron spin echo – high E resolution

Lecture on Thursday

~30 %

Spherical neutron polarimetry

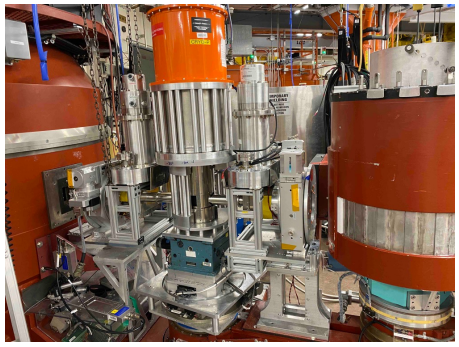

Full polarization analysis including off-diagonal terms

Detailed magnetic structure
Chirality
Nuclear-magnetic interference

Lecture on Wednesday

~10 %

Helmholtz coils (5 independent coils)
- Controlling magnetic field along arbitrary directions -

2 coils for vertical field

3 coils for horizontal field

Cross section

M. Blume, Phys. Rev. 130, 1670 (1963)

$$\frac{d\sigma}{d\Omega} = NN^* + N^*(\mathbf{P}_i\cdot\mathbf{M}_\perp) + N(\mathbf{P}_i\cdot\mathbf{M}^*_\perp) + \mathbf{M}_\perp\cdot\mathbf{M}^*_\perp + i\mathbf{P}_i\cdot(\mathbf{M}^*_\perp \times \mathbf{M}_\perp)$$

nuclear

interference

magnetic

chirality

Polarization vector of scattered neutrons

$$\mathbf{P}_f\frac{d\sigma}{d\Omega} = \mathbf{P}_i NN^* + \mathbf{M}_\perp N^* + \mathbf{M}^*_\perp N - i(\mathbf{P}_i \times \mathbf{M}_\perp N^* - \mathbf{P}_i \times \mathbf{M}^*_\perp N) + \mathbf{M}_\perp(\mathbf{P}_i\cdot\mathbf{M}^*_\perp) + \mathbf{M}^*_\perp(\mathbf{P}_i\cdot\mathbf{M}_\perp) - \mathbf{P}_i(\mathbf{M}_\perp\cdot\mathbf{M}^*_\perp) + i(\mathbf{M}^*_\perp \times \mathbf{M}_\perp)$$

nuclear

interference

magnetic

chirality

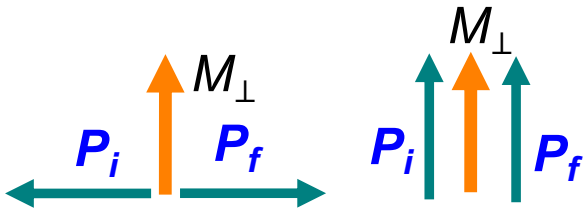

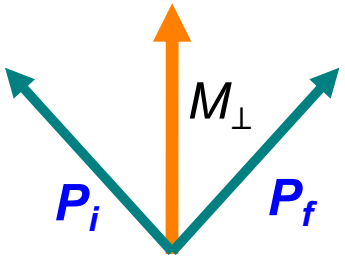

Precession of 180° around $M_\perp$

Half polarized experiments with single crystals

Cryomagnet - ferromagnetism

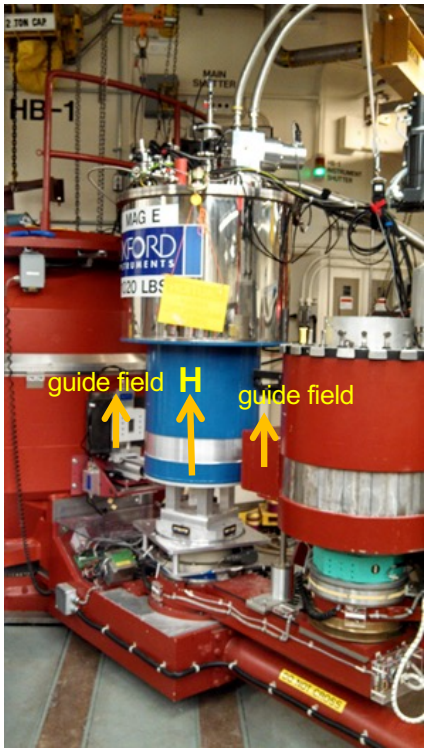

Helmholtz coils - helicity ($S_n \perp$ helical plane)

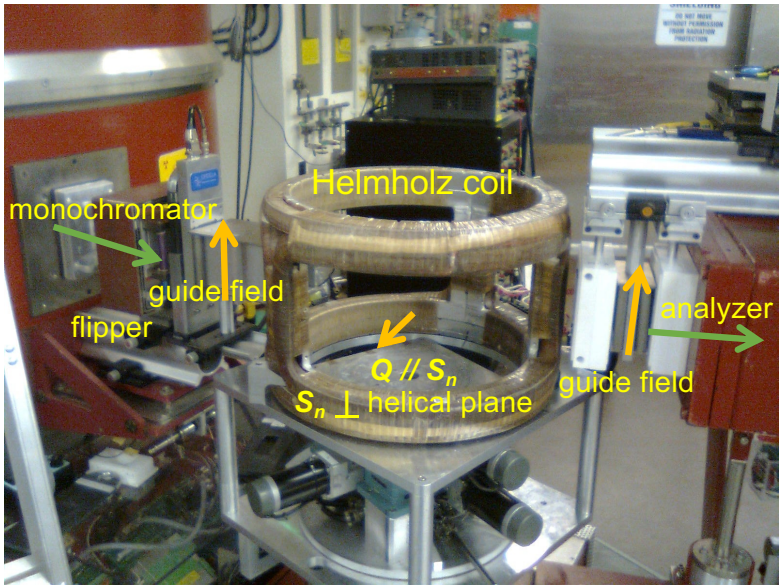

Experimental setup

Heusler monochromator – flipper (+ or -) – sample – PG or no analyzer
PG monochromator – sample – flipper (+ or -) – Heusler analyzer

Half polarization analysis of weak ferromagnetic component

$I_{\pm} = (F_N \pm F_M)^2$ $\quad$ +: $\boldsymbol{S}_N$ // $\boldsymbol{H}$; - : $\boldsymbol{S}_N$ // $-\boldsymbol{H}$

F_N: nuclear structure factor
F_M: ferromagnetic structure factor

Flipping ratio $\quad R = \dfrac{(F_N + F_M)^2}{(F_N - F_M)^2}$

For $F_M << F_N$ $\quad R \sim 1+4\dfrac{F_M}{F_N}$ $\quad$ (R ~1.4 for F_M/F_N=0.1)

Intensity ratio for unpolarized neutrons $\quad \dfrac{F_M^2}{F_N^2}$ $\quad$ (~0.01 for F_M/F_N=0.1)

Ferromagnetic component in Wyle semimetal $Co_3Sn_2S_2$

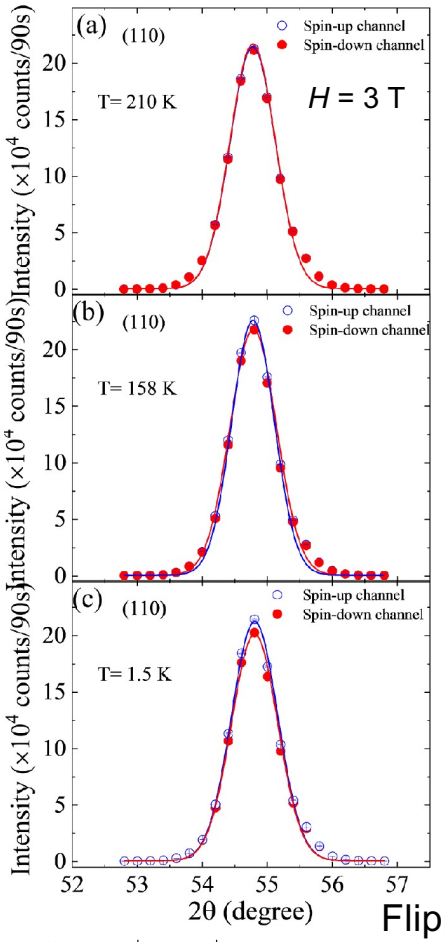

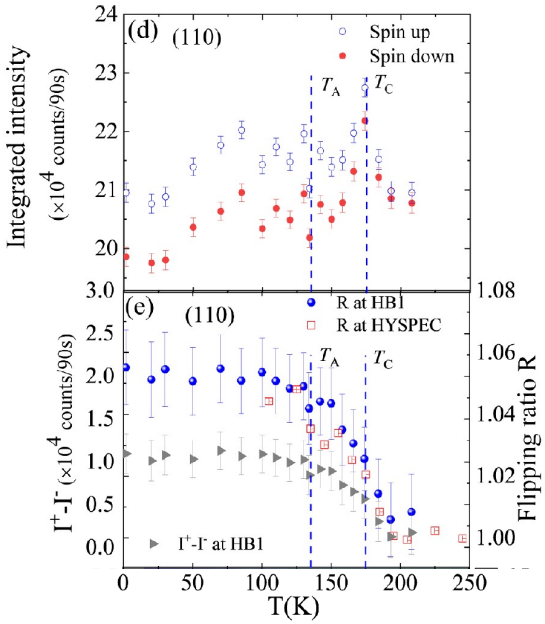

$I_{\pm} = (F_N \pm F_M)^2$

$I_+ - I_- = 4F_N \cdot F_M$

$R = 1 + 4F_M/F_N$

Flipping ratio ~ 1.055 F_M/F_N=0.0172

F_M^2/F_N^2=0.0003

Q. Zhang *et al.*, JACS 144, 14339 (2022)

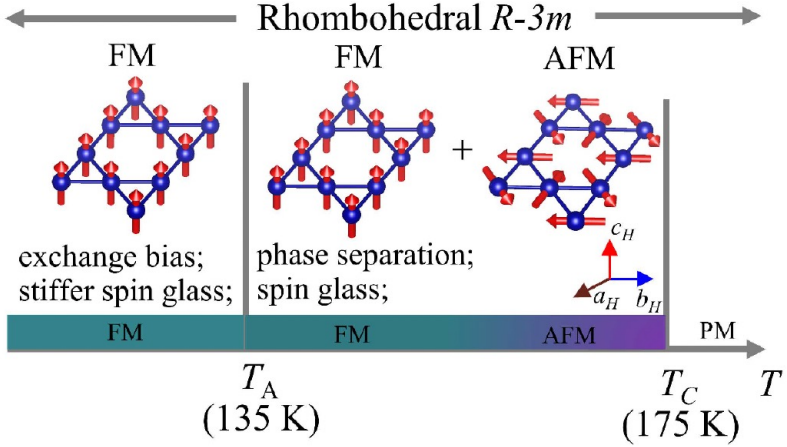

- **0.14(2) μ_B at 1.5 K**
- **No long-range AFM phase**

Canted magnetic structure in $^{154}SmRu_4P_{12}$

T. Matsumura *et al.*, Phys. Rev. B 102, 214444 (2020)

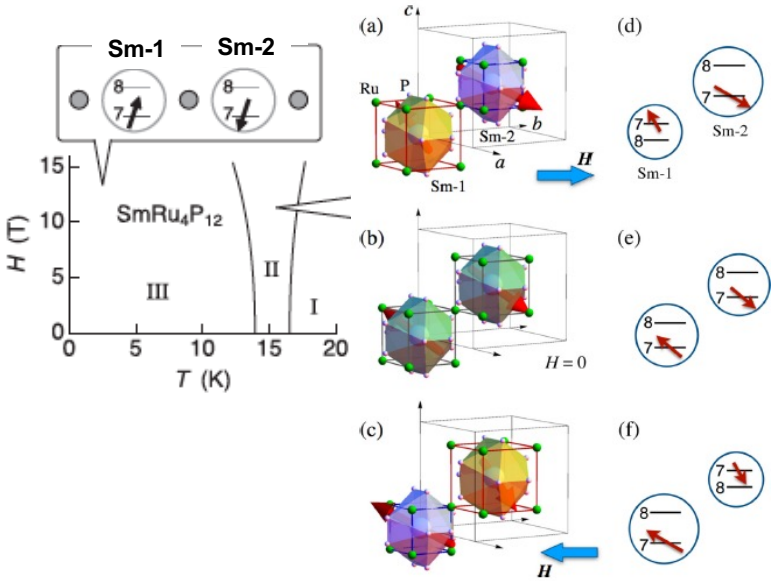

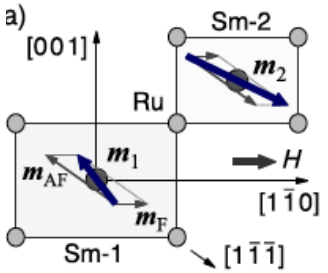

Sample volume < 1 mm^3
m_{AF}=0.16 μ_B
m_F=0.06 μ_B

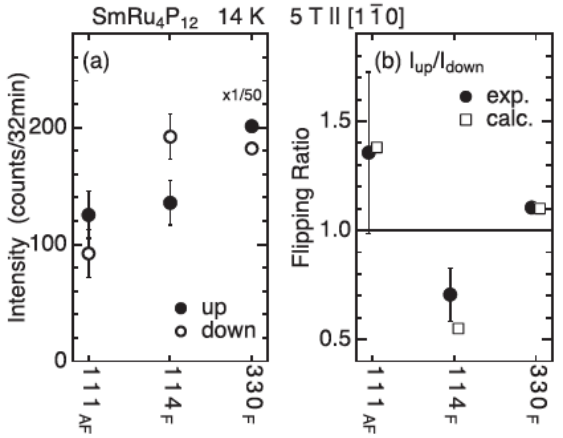

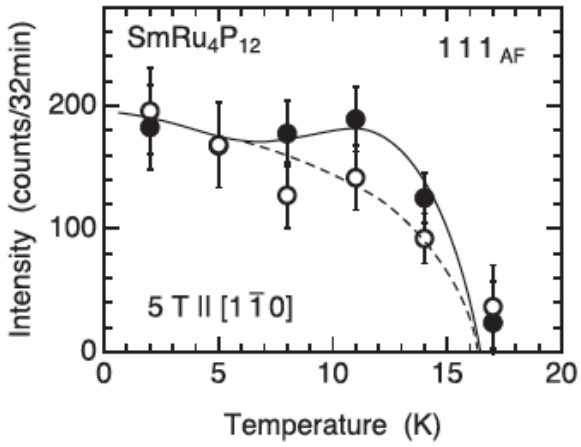

Intermediate phase (phase II)

Field-induced CDW caused by *p-f* hybridization

m_1 (m_2) reduced (increased) with surrounding cage expanded (shrunk)

Consistent with resonant x-ray diffraction data

Magnetic structure of ferromagnetic thin film $Fe_{16}N_2$

X. Hang *et al.*, Phys. Rev. B 102, 104402 (2020)
X. Hang, PhD Dissertation, Univ. of Minnesota (2021)

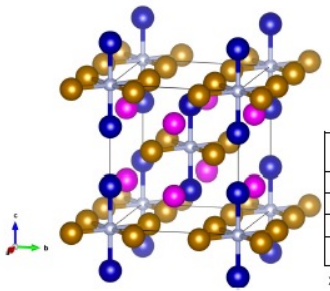

	Wyckoff pos.	Atomic pos.
N	2a	(0, 0, 0)
Fe(1)	4e	(0, 0, z)
Fe(2)	8h	(x, x, 0)
Fe(3)	4d	$(0, \frac{1}{2}, \frac{1}{4})$

x = 0.2449, z = 0.2898

FIG. 1. Crystal structure of $Fe_{16}N_2$.

$Fe_{16}N_2$: giant saturation magnetization

Difficult powder sample preparation (ferromagnetic impurities)

Thin films (on MgO)
1 in. X 1 in. X 40 nm
10 pieces

room temperature H=3 T

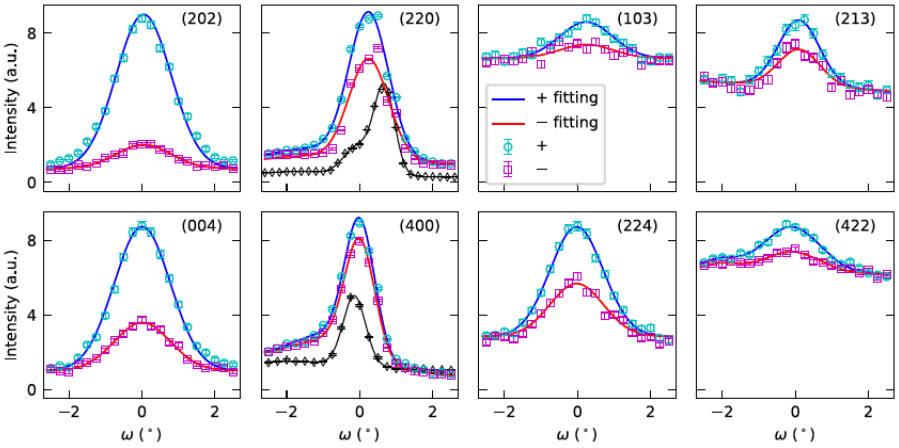

Model	m_1 (μ_B)	m_2	m_3	M_s (emu/cm^3)	χ^2
Min [30]	2.13	2.50	2.85	1800 (2.26)	20
Lai [31]	2.36	2.75	3.53	2050 (2.58)	6.6
Huang [32]	2.06	2.42	2.90	1770 (2.22)	22
Sakuma [33]	2.27	2.25	2.83	1730 (2.17)	25
Tanaka [34]	2.17	1.95	2.74	1590 (2.00)	37
Ji [42][a]	3.1	3.25	2.7	2220 (2.79)	3.2
Sims [35][b]	2.83	2.91	3.08	2110 (2.66)	5.1
Ke [36][b]	2.24	2.55	3.12	1890 (2.37)	15
Szymanski [37]	2.74	2.82	2.96	2040 (2.57)	7.4
Hiraka [38]	1.4	1.8	2.6	1370 (1.72)	60

Fe(1)	Fe(2)	Fe(3)	m_1	m_2	m_3
Fe^0	Fe^{3+}	Fe^{1+}	2.8 ± 0.3	3.8 ± 0.2	1.6 ± 0.5
Fe^{1+}	Fe^{3+}	Fe^0	3.1 ± 0.3	3.9 ± 0.2	1.1 ± 0.4
Fe^{1+}	Fe^{3+}	Fe^{1+}	3.1 ± 0.3	3.8 ± 0.2	1.6 ± 0.5
Fe^{2+}	Fe^{3+}	Fe^{1+}	2.7 ± 0.3	3.8 ± 0.2	1.6 ± 0.5
Fe^{3+}	Fe^{3+}	Fe^{1+}	2.4 ± 0.3	3.7 ± 0.2	1.7 ± 0.5

Magnetic form factor of Ru^{3+} in α-$RuCl_3$

Observation of field-induced moment in the paramagnetic phase

C. L. Sarkis *et al.*, Phys. Rev. B 109, 104432 (2024)

Single crystal: 2 g

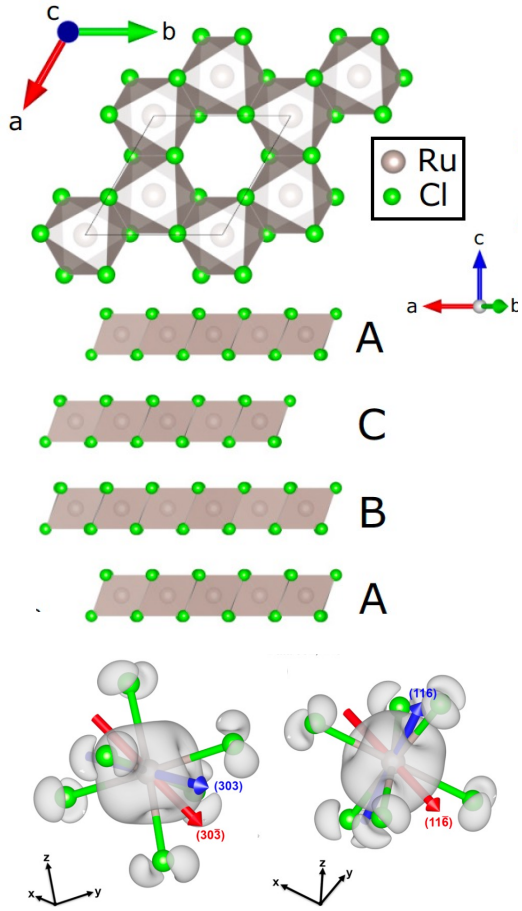

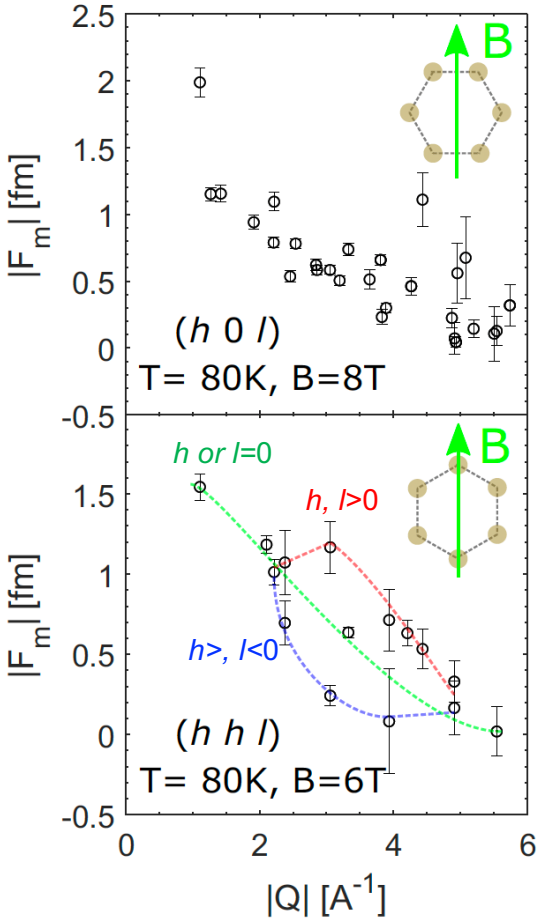

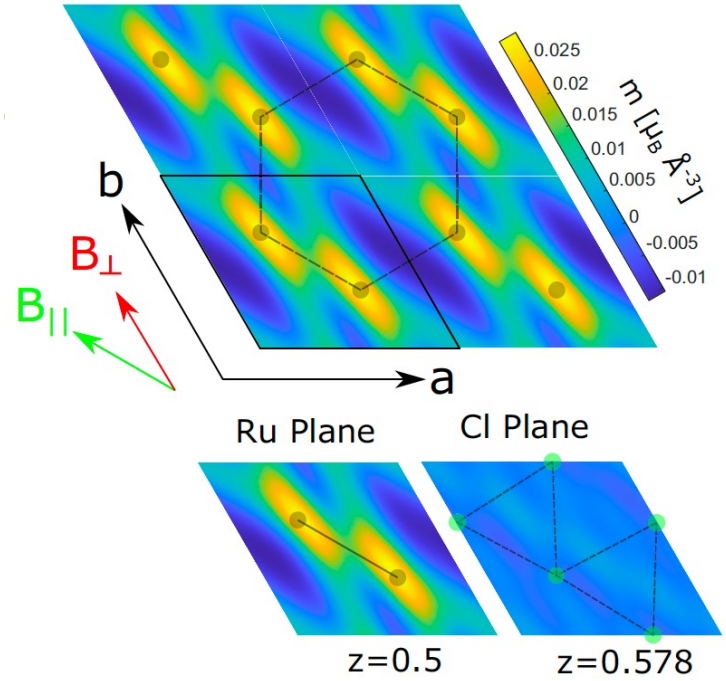

Magnetization density of Ru and Cl

Hybridization between Ru and Cl

Half polarization analysis of helicity

Magnetic intensities of incommensurate peak at Q $\pm$ δ

$$\left(\frac{d\sigma}{d\Omega}\right)^{\pm} = I_0\{m_b^2 + m_c^2 \pm 2m_b m_c(\hat{S}_n \cdot \hat{C})\}$$

m_b: spin component along *b*
m_c: spin component along *c*
S_n: neutron spin vector
C: chirality vector

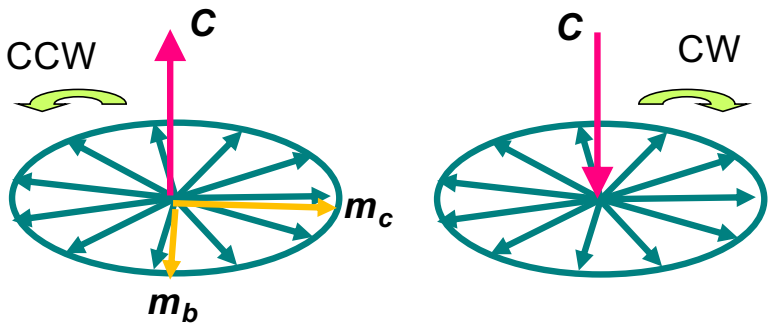

$m_b = m_c$ and S_n // C → $I^+ = 4m_b^2$
$m_b = m_c$ and S_n // $-C$ → $I^- = 0$

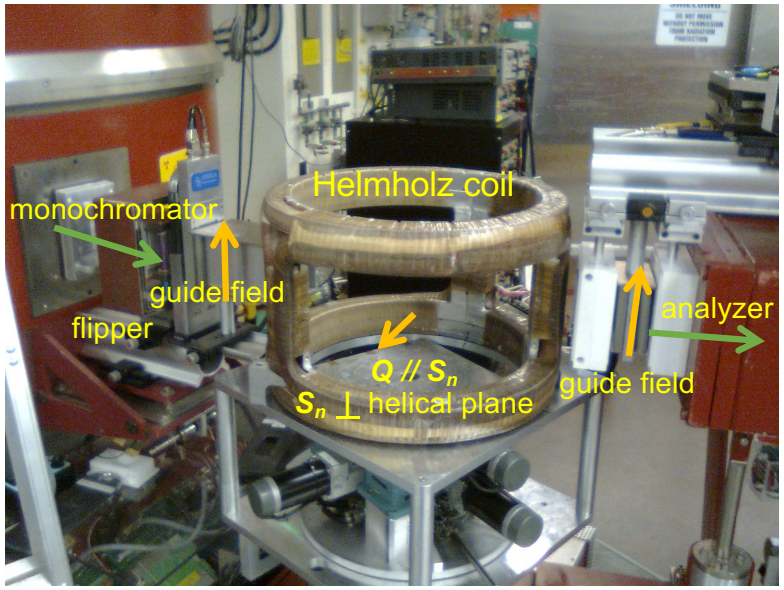

Chirality in ferro-rotational material $RbFe(SO_4)_2$ - multiferroic behavior -

J. Yang et al., Adv. Sci. 11, 2402048 (2024)

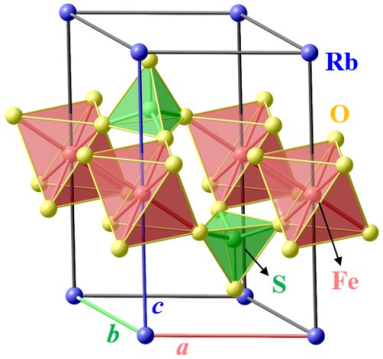

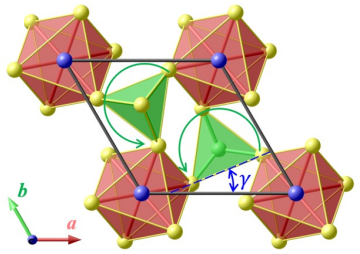

CCW domain
γ: positive

Helical order below 4 K

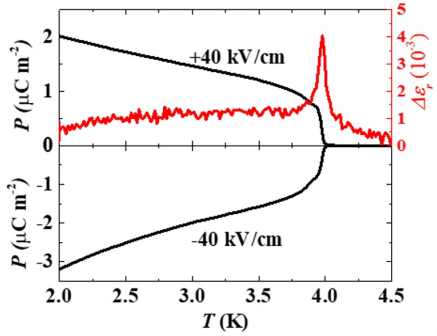

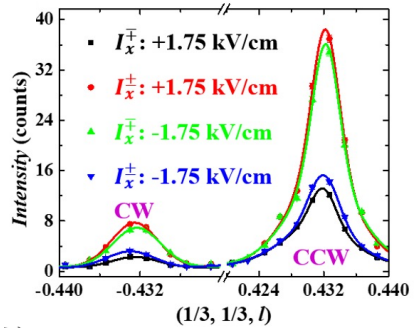

Dominant CCW domain

$$\left(\frac{d\sigma}{d\Omega}\right)^{\pm} = I_0\{m_{//}^2 + m_{\perp}^2 \pm 2m_{//}m_{\perp}(\hat{S}_n \cdot \hat{C})\}$$

Single crystal: 3 X 3 X 1 mm^3
Moment: ~3μ_B

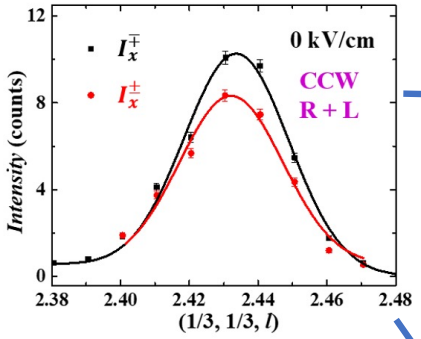

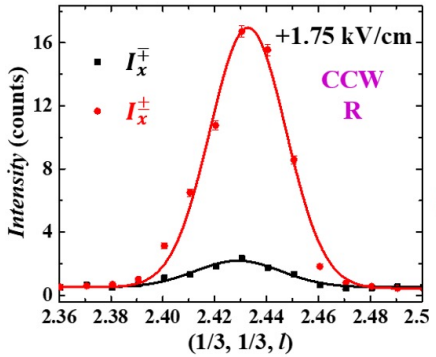

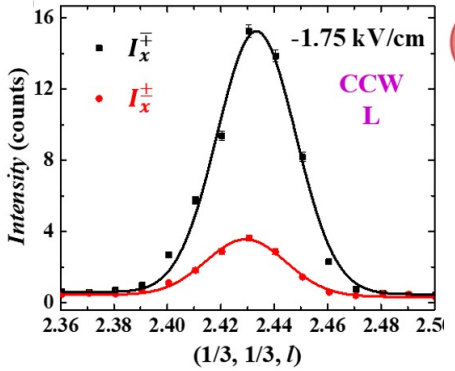

Right-handed

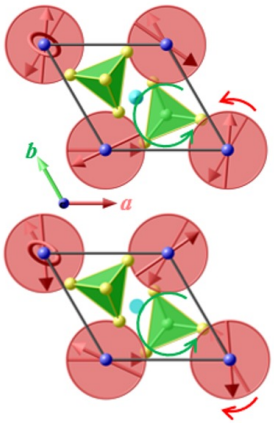

Left-handed

Controlling helical domain with electric field

Skyrmion-lattice phase in EuPtSi

K. Kaneko et al., J. Phys. Soc. Jpn. 88, 013702 (2019)

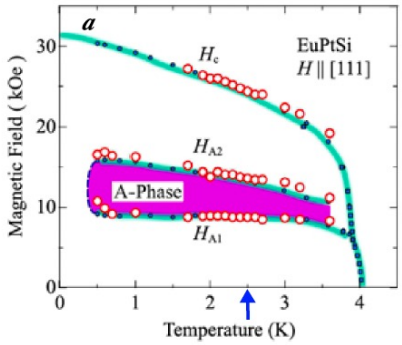

A-phase: skyrmion-lattice

q_A=(-0.09, -0.20, 0.28)

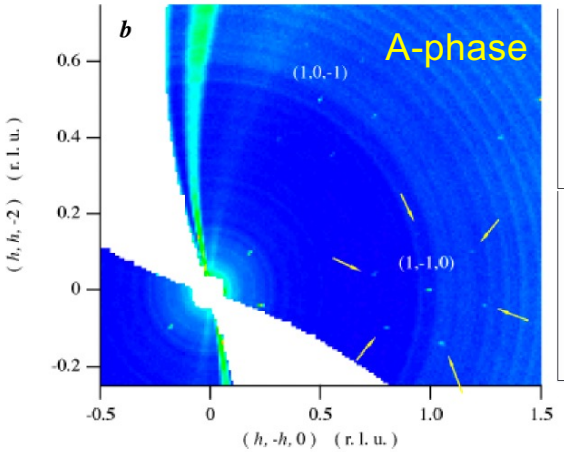

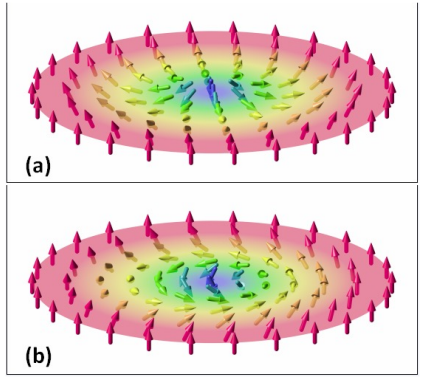

unpolarized neutron

Magnetic ground state at ambient field

q=(0.00, -0.20, 0.30) at 1.5 K

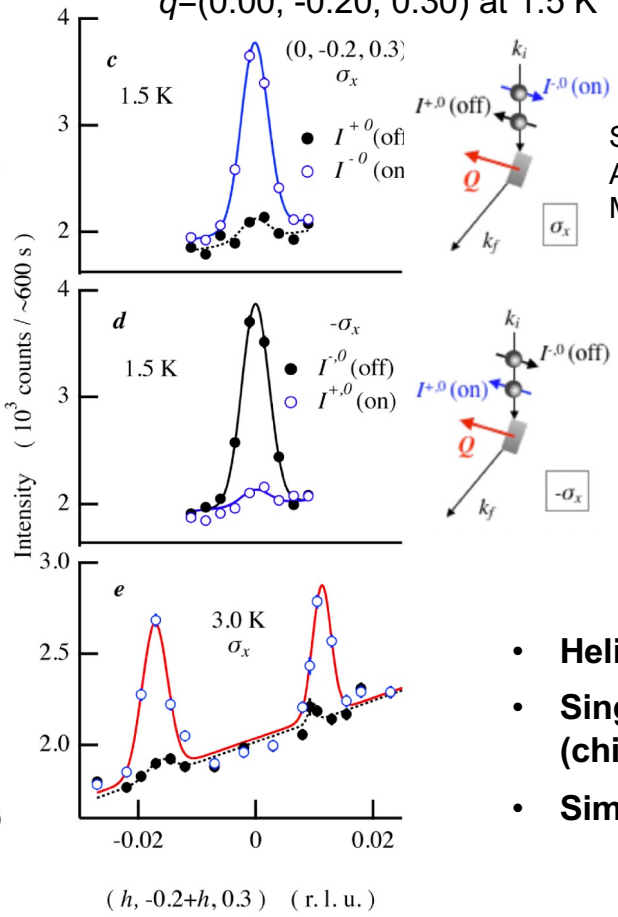

Single crystal: 2 X 2 X 1 mm^3
Absorption by Eu
Moment: S=7/2

- **Helical structure**
- **Single helical domain (chiral crystal structure)**
- **Similar to MnSi**

Summary

Half polarization analysis (diffraction with single crystals)

- Sensitive to tiny ferromagnetic component

- Helicity

  Presence of helicity

  Helical domain ratio (CW and CCW)

  Ellipticity

  complementary to SNP

Cross section

M. Blume, Phys. Rev. 130, 1670 (1963)

$$\frac{d\sigma}{d\Omega} = NN^* + N^*(\mathbf{P}_i\cdot\mathbf{M}_\perp) + N(\mathbf{P}_i\cdot\mathbf{M}^*_\perp) + \mathbf{M}_\perp\cdot\mathbf{M}^*_\perp + i\mathbf{P}_i\cdot(\mathbf{M}^*_\perp \times \mathbf{M}_\perp)$$

nuclear

interference

magnetic

chirality

Polarization vector of scattered neutrons

$$\mathbf{P}_f\frac{d\sigma}{d\Omega} = \mathbf{P}_i NN^* + \mathbf{M}_\perp N^* + \mathbf{M}^*_\perp N - i(\mathbf{P}_i \times \mathbf{M}_\perp N^* - \mathbf{P}_i \times \mathbf{M}^*_\perp N) + \mathbf{M}_\perp(\mathbf{P}_i\cdot\mathbf{M}^*_\perp) + \mathbf{M}^*_\perp(\mathbf{P}_i\cdot\mathbf{M}_\perp) - \mathbf{P}_i(\mathbf{M}_\perp\cdot\mathbf{M}^*_\perp) + i(\mathbf{M}^*_\perp \times \mathbf{M}_\perp)$$

nuclear

interference

magnetic

chirality

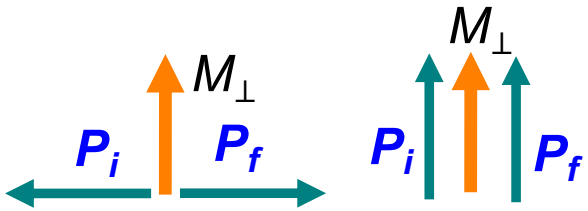

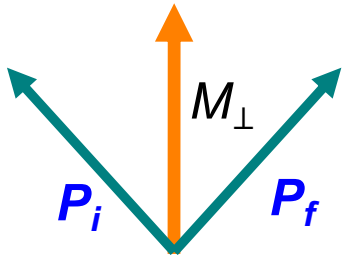

Precession of 180° around $M_\perp$

Linear-polarization analysis with Helmholtz coils

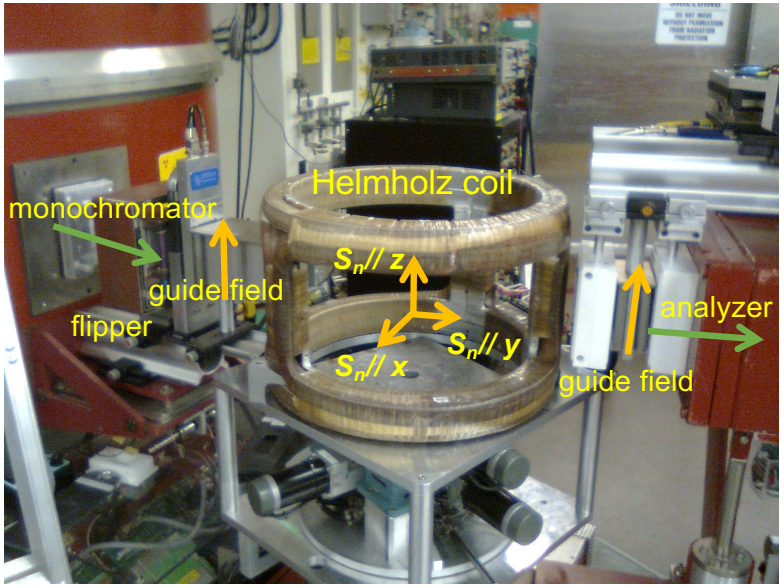

S_N // Q (x) NSF: nuclear
SF: magnetic ($S_y^2+S_z^2+P_iS_{chiral}$)

$S_N \perp$ Q (z) NSF: nuclear + magnetic (S_z^2)
SF: magnetic (S_y^2)

$S_N \perp$ Q (y) NSF: nuclear + magnetic (S_y^2)
SF: magnetic (S_z^2)

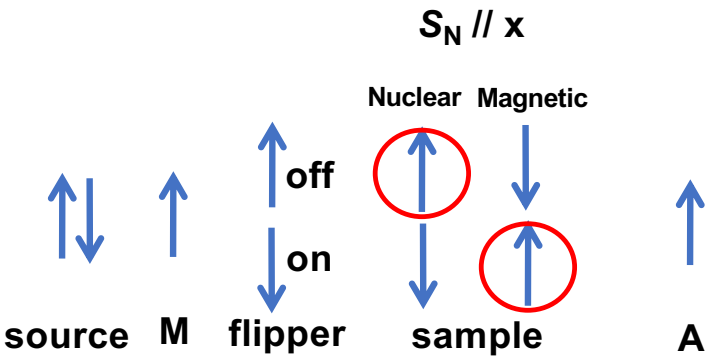

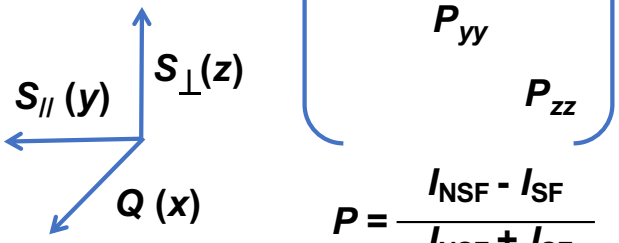

$$\begin{pmatrix} P_{xx} & & \\ & P_{yy} & \\ & & P_{zz} \end{pmatrix}$$

$$P = \frac{I_{NSF} - I_{SF}}{I_{NSF} + I_{SF}}$$

Linear-polarization analysis with vertical field cryomagnet

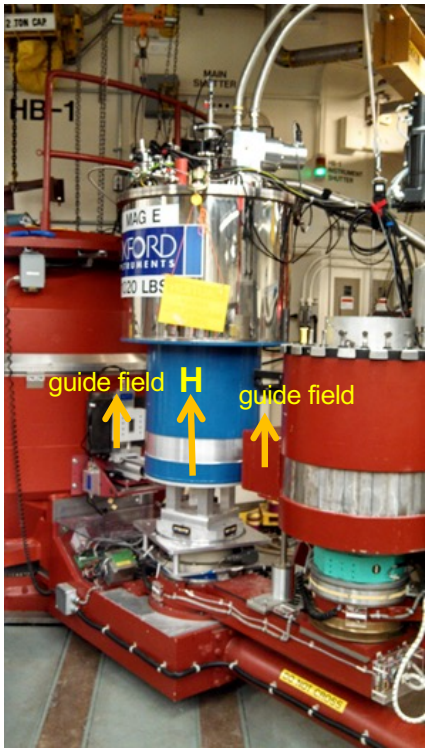

8T vertical field magnet

Study of ferromagnets
Study of magnetic-field-induced phase

Only P_{zz} is observable.

$S_N \perp$ scattering plane (z)

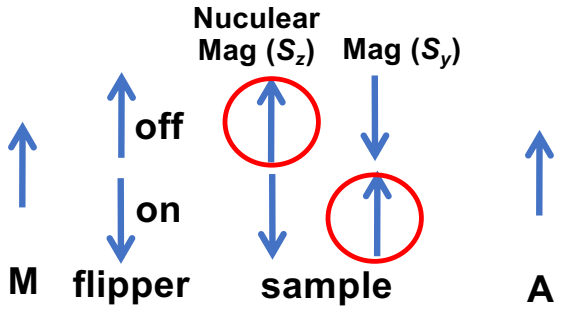

Horizontal field magnet with S_N // Q to observe P_{xx} (unavailable on PTAX)

Linear-polarization analysis

- **Powder diffraction**

  Separating nuclear and magnetic contributions

- **Single crystal diffraction**

  Separating nuclear and magnetic contributions

  Determining spin directions in detail

Determining magnetic structure of Ir in pyrochlore $Nd_2Ir_2O_7$ Helmholtz coils

Polarized neutron powder diffraction

sample: 4.8 g
annular holder: 20 mmϕ and 0.8 mm thickness

K. Tomiyasu *et al.*, Sci. Rep. 8, 16228 (2018)

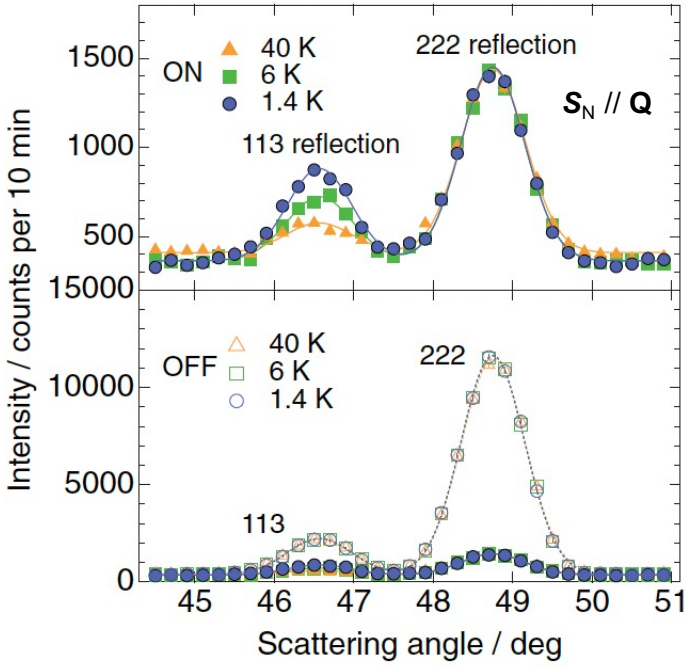

- **Magnetic / nuclear intensities overlap.**
- **Polarized beam reduces relative nuclear intensities by ~15.**

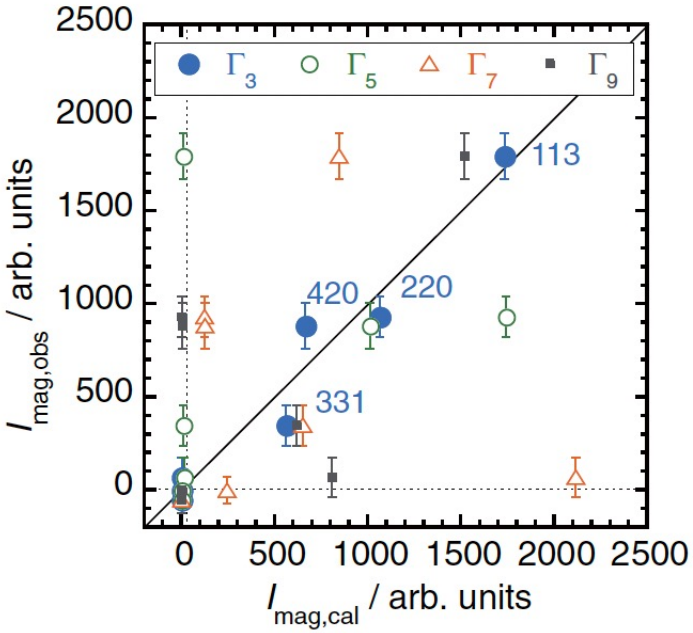

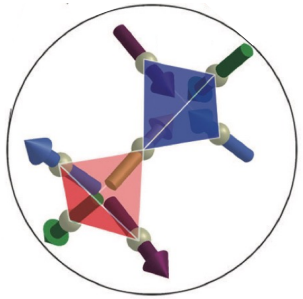

- **Γ_3 (all-in / all-out) is best.**
- **m_{Ir} = 0.14(5) μ_B and m_{Nd} = 1.22(5) μ_B at 1.4 K**

Separating magnetic and nuclear components in single crystal

Magnetic structure in Rh-doped Sr_2IrO_4 Helmholtz coils

F. Ye et al., PRB 92, 201112(R) (2015)

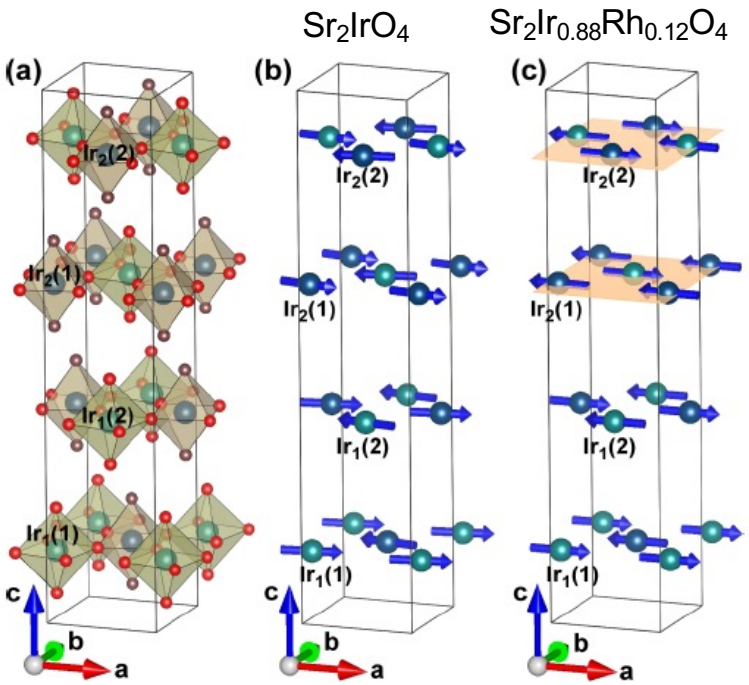

$Sr_2Ir_{0.88}Rh_{0.12}O_4$

small crystal (2 X 2 X 0.5 mm^3, ~10 mg)
0.18 μ_B / Ir
Ir absorption

unpolarized **polarized (S_N // Q)**

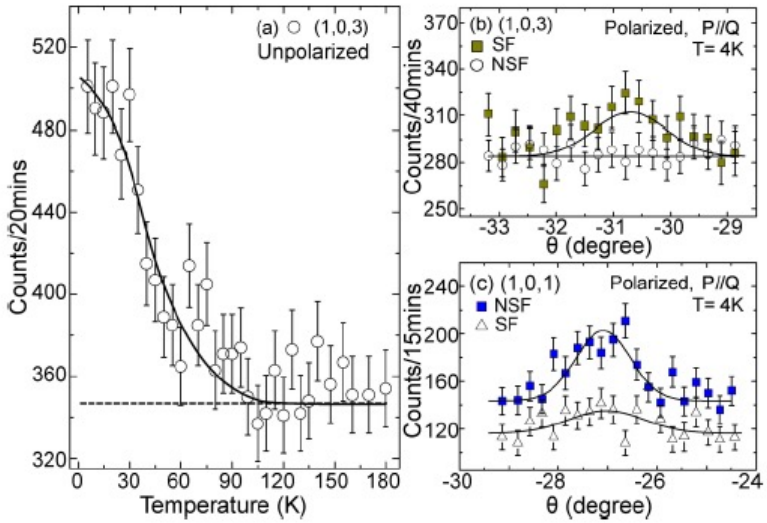

(103) is magnetic.
(101) is nuclear.

Detailed magnetic structure in 4f-electron system NdB_4

Helmholtz coils

N. Metoki et al., PRB 97, 174416 (2018)

	S_N // Q		$S_N \perp Q$ (z)	
	HF-NSF	HF-SF	VF-NSF	VF-SF
$(H,K,0)$			b, m_c	$m_{\perp c}$
$(H,0,L)$	b	$m_c, m_{\perp c}$	$b, (m_{\perp c})_{ver.}$	$m_c, (m_{\perp c})_{hor.}$
(H,H,L)			$b, (m_{\perp c})_{ver.}$	$m_c, (m_{\perp c})_{hor.}$

(a) Γ_4 (all-in all-out) (b) Γ_5 (diagonal FM)

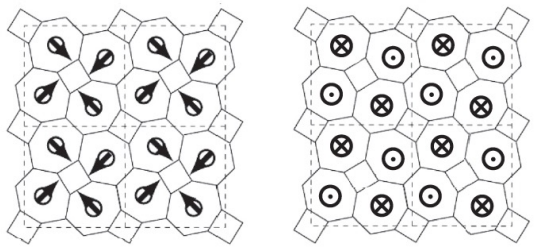

(c) Γ_{10} (diagonal AFM) (d) Γ_3 (FM)

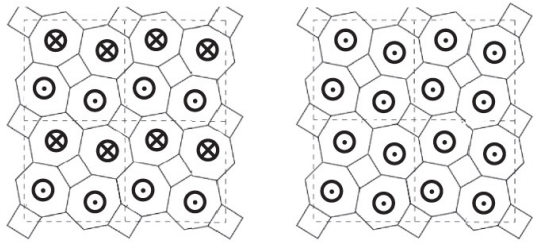

crystal: 4 X 2 X 2 mm³

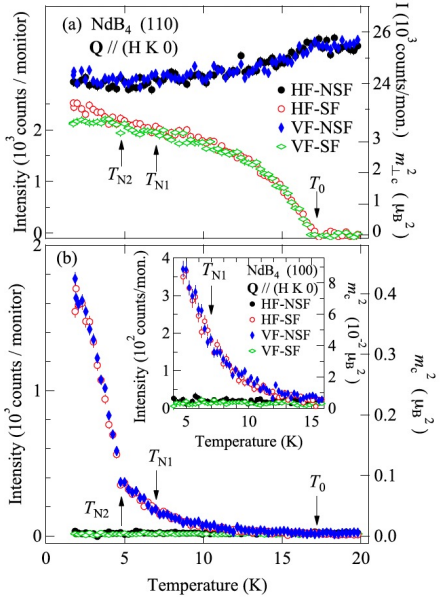

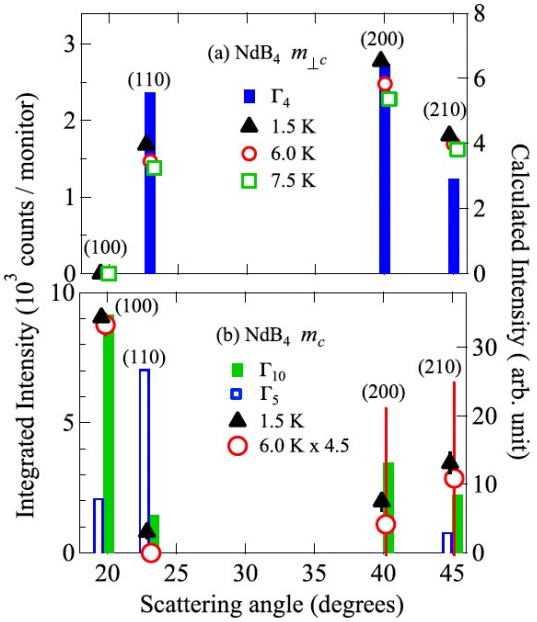

- **ab-plane and c-axis spin components behave independently.**
- **ab-plane: Γ_4 and c-axis: Γ_{10}**

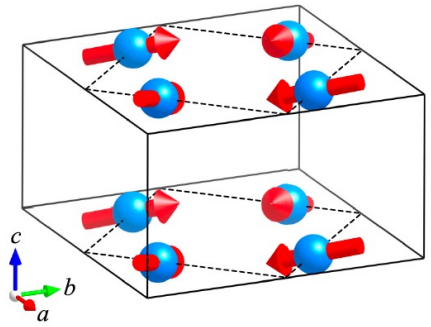

Helical spin structure in MnP under high pressure

Helmholtz coils

M. Matsuda et al., Physica B 551, 115 (2018)

(a) helical *c*

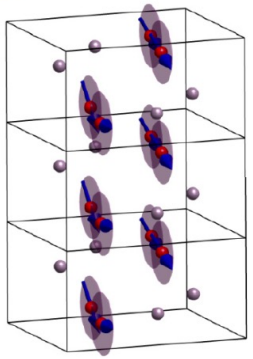

(b) helical *b*

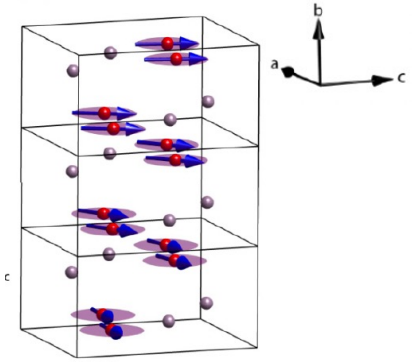

helical c (0 GPa) crystal: 5 X 3 X 2 mm³

Half-polarization

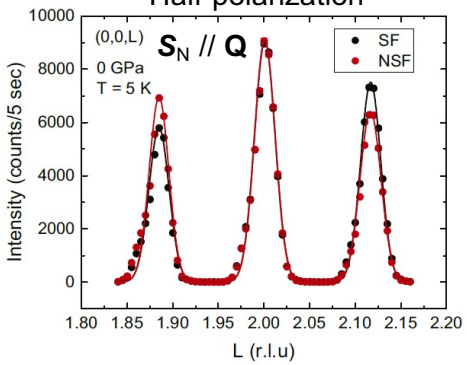

Full-polarization

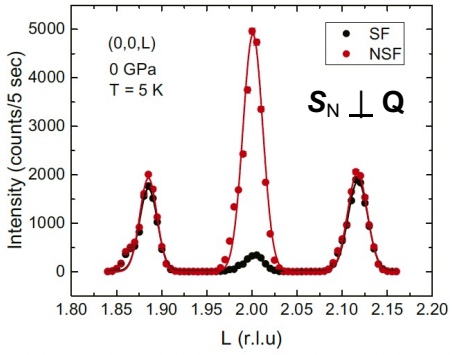

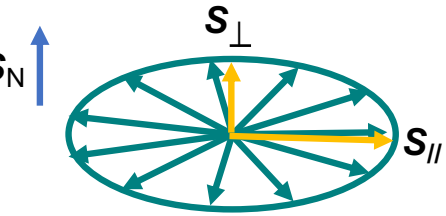

(*H0L*)
SF: S_a^2
NSF: S_b^2

helical b (1.8 GPa) crystal: 1 X 1 X 3 mm³

Half-polarization

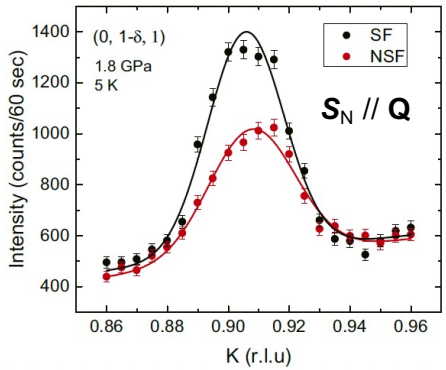

Full-polarization

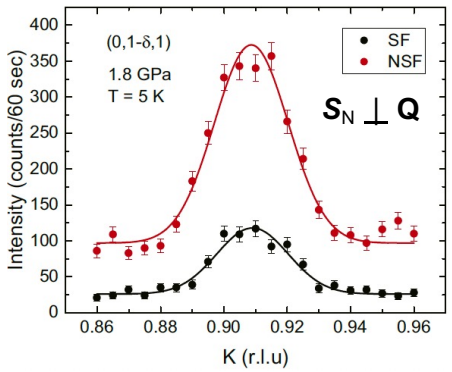

(0*KL*)
SF: S_c^2
NSF: S_a^2

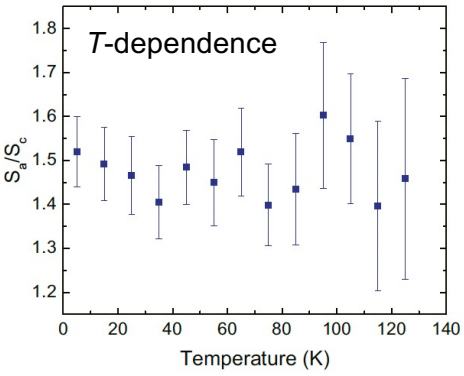

Helical structure

- **Half-polarization: presence of helicity, helical domain ratio**
- **Full-polarization: ellipticity, out-of-plane component (spin canting)**

Polarized inelastic neutron measurements

- Separating magnons and phonons
- Mode analysis of magnetic excitations (longitudinal or transverse mode)

Separating magnon and phonon in multiferroic (La,Ca)MnO_3 cryomagnet

J. Fernandez-Baca, F. Ye et al., in preparation

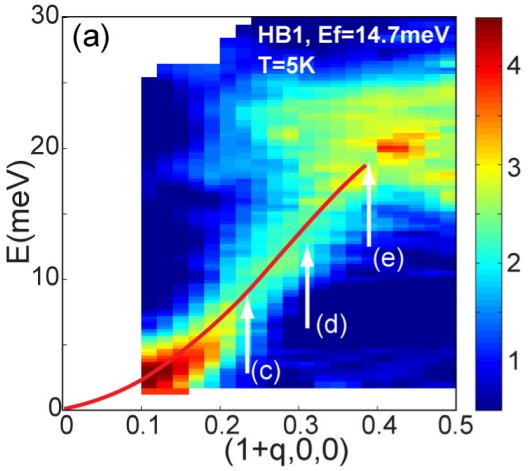

Unpolarized results at HB-1

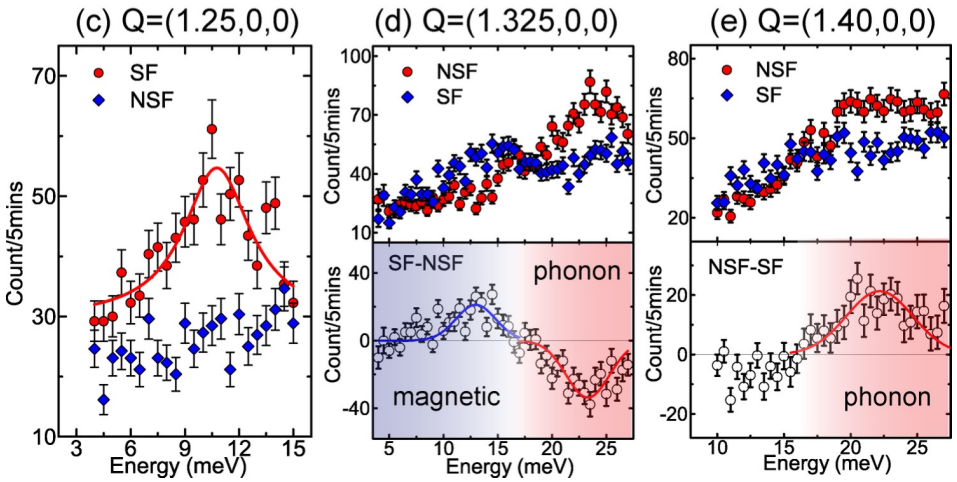

$S_N \perp Q$

Polarized results at HB-1 (HK0) plane
H(=3T) // c-axis (to align magnetic domains)
SF: magnon (transverse)
NSF: phonon + ~~magnon (longitudinal)~~

- Magnon < 17 meV
- Phonon > 17 meV

Mode analysis of spin-wave excitations in multiferroic $Ba_2Mg_2Fe_{12}O_{22}$ cryomagnet

$Ba_2Mg_2Fe_{12}O_{22}$ (multiferroic material)

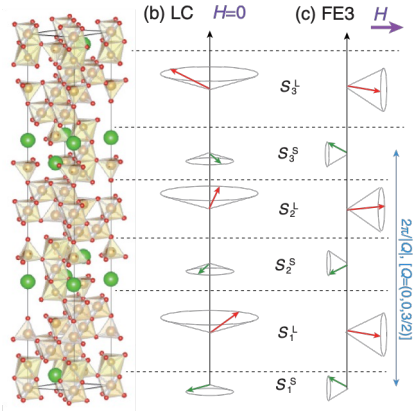

time-domain THz spectra

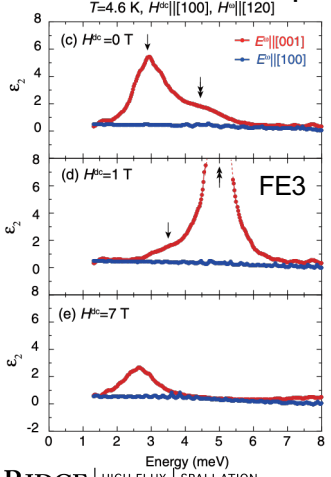

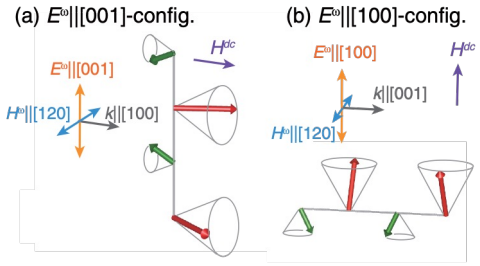

electromagnon

T. Nakajima et al., PRB 93, 035119 (2016)

unpolarized **1.81 g crystal** **polarized** $S_N \perp Q$

H = 1 T (FE3 phase)

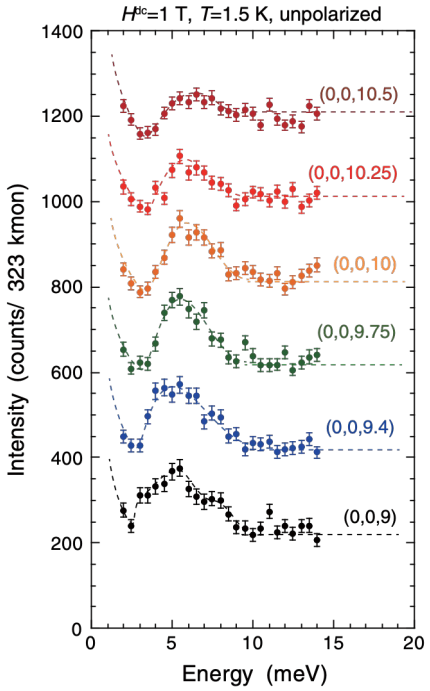

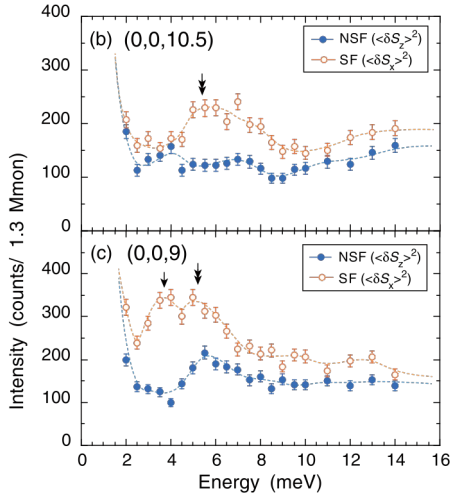

NSF $z \parallel [100]$, H^{dc}, p_N

SF $x \parallel [120]$, b^* $y \parallel c$

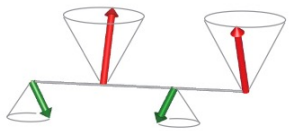

Magnon mode in cycloidal plane!

Mode analysis of magnetic excitations in 5f heavy fermion system UPt_2Si_2

Helmholtz coils

J. Lee et al., PRL 121, 057201 (2018)

Unpolarized data measured on SEQUOIA

T_N = 32 K
moment // c
~ 2 μ_B

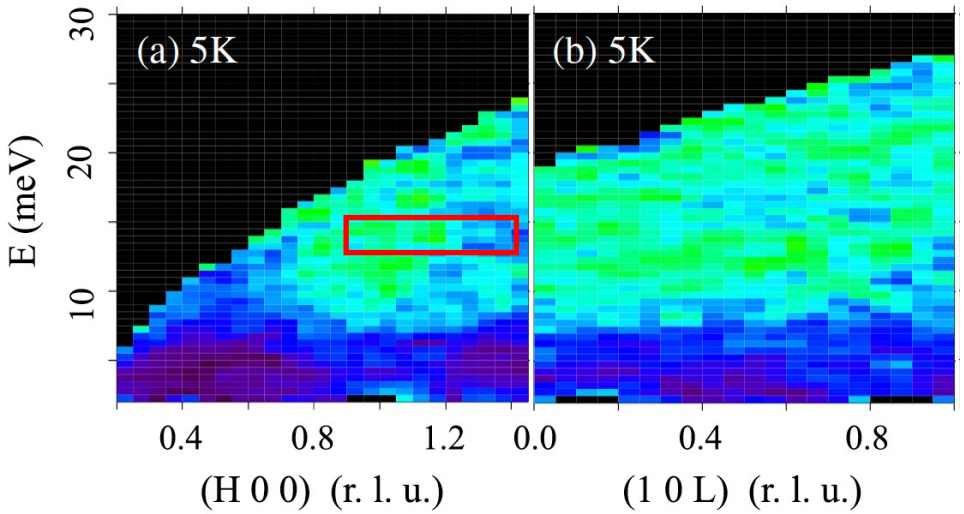

- **Broad continuum characteristic of itinerant system**
- **Transverse magnetic fluctuations characteristic of localized system**
- **Dual nature of magnetism**

Polarization analysis on PTAX

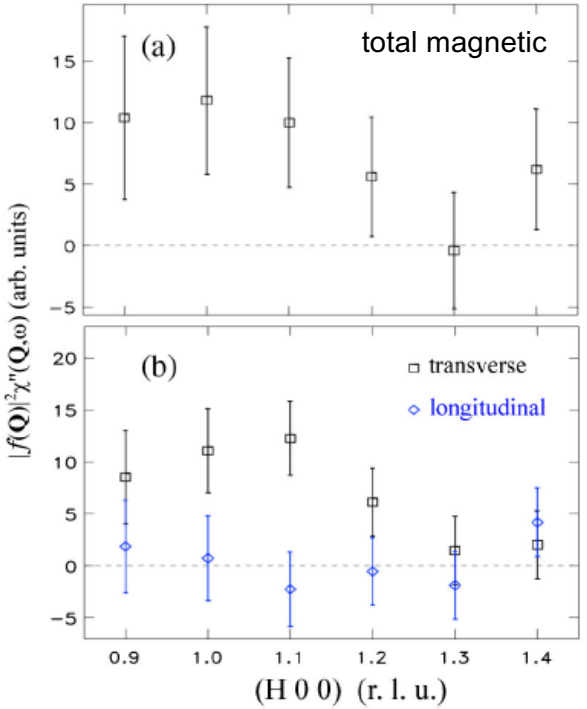

1.5 g crystal

(*H*0*L*) scattering plane

(*H*00) S_N // ***a*** **and SF:** $m_b^2+m_c^2$
S_N // ***b*** **and NSF:** m_b^2 **(transverse)**
S_N // ***b*** **and SF:** m_c^2 **(longitudinal)**

Mode analysis of magnetic excitations in multiferroic $BiFeO_3$ - complementary use of HYSPEC and PTAX -

Helmholtz coils

HYSPEC (SNS) D. Zhang, B. Winn, M. Matsuda et al., PRB 105, 144426 (2022)

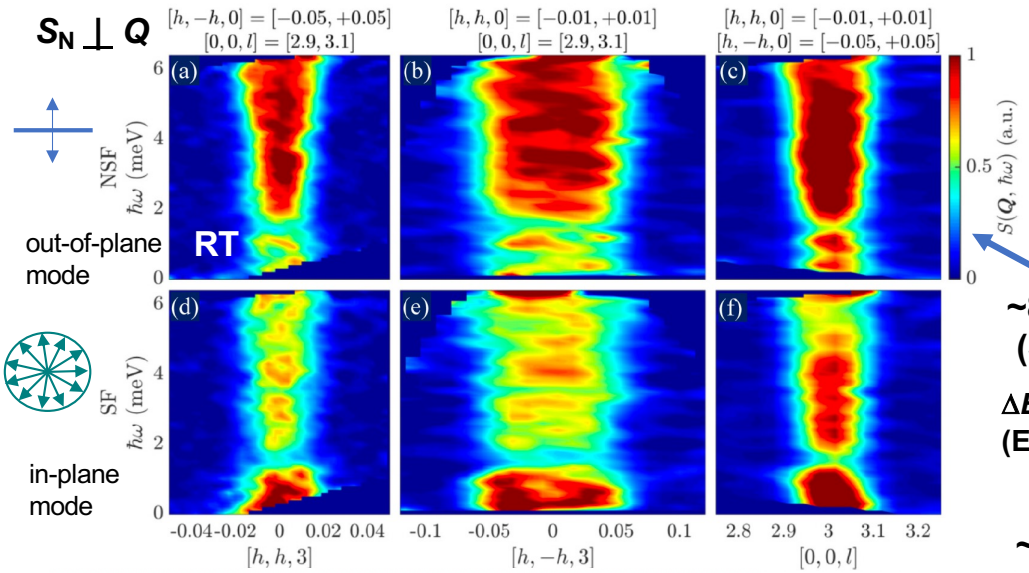

~80 hours (SF+NSF)

ΔE~0.5 meV (Ei=7.5 meV)

~40 hours (~7 hrs/energy)

ΔE~1.5 - 2 meV Ef=13.5 meV

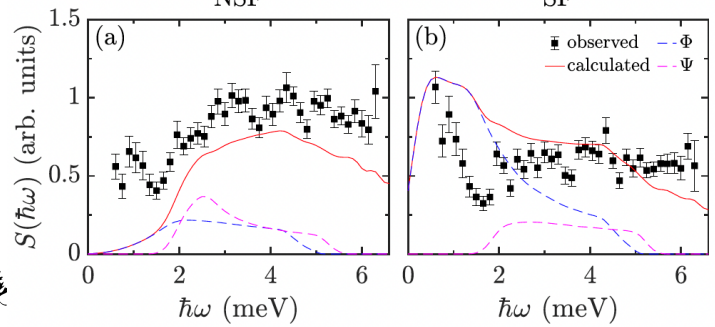

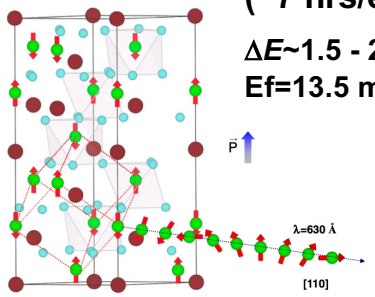

PTAX (HFIR) M. Matsuda et al., J. Phys.:Conf. Ser. 2481, 012003 (2023)

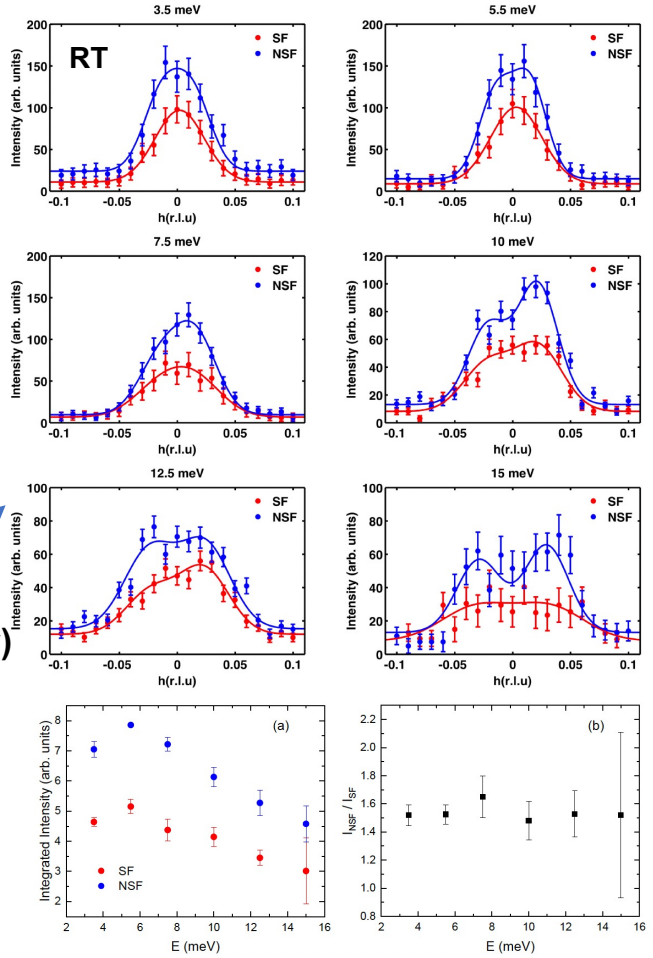

Summary

Linear polarization analysis on PTAX

- Diffraction
  Separating magnetic and nuclear components
  Spin directions (single crystal)

- Inelastic scattering
  Separating magnons and phonons
  Mode analysis of magnetic excitations (single crystal)